First results from the ESO slice project (ESP) galaxy redshift survey

E. ZUCCA[1], G. VETTOLANI[1], A.CAPPI[2], R. MERIGHI[2], M. MIGNOLI[2],
G. STIRPE[2], G. ZAMORANI[2], H. MacGILLIVRAY[3], C. COLLINS[4],
C. BALKOWSKI[5], J. ALIMI[5], V. CAYATTE[5], P. FELENBOK[5],
S. MAUROGORDATO[5], D. PROUST[5], G. CHINCARINI[6], L. GUZZO[6],
D. MACCAGNI[7], R. SCARAMELLA[8], A. BLANCHARD[9], M. RAMELLA[10]

[1] *Istituto di Radioastronomia del CNR, Bologna, Italy*
[2] *Osservatorio Astronomico di Bologna, Bologna, Italy*
[3] *Royal Observatory Edinburgh, Edinburgh, United Kingdom*
[4] *Liverpool John Moores University, Liverpool, United Kingdom*
[5] *DAEC, Observatoire de Paris–Meudon, Meudon, France*
[6] *Osservatorio Astronomico di Brera, Milano, Italy*
[7] *Istituto di Fisica Cosmica e Tecnologie Relative, Milano, Italy*
[8] *Osservatorio Astronomico di Roma, Monteporzio Catone, Italy*
[9] *Universitè Louis Pasteur, Strasbourg, France*
[10] *Osservatorio Astronomico di Trieste, Trieste, Italy*

The ESO Slice Project (ESP) is a galaxy redshift survey we are accomplishing as an ESO Key–Project over about 30 square degrees, in a region near the South Galactic Pole. The limiting magnitude is b_J=19.4. Observations were completed in October 1994 and all the obtained data were reduced, providing 3348 galaxy redshifts. We present some preliminary results concerning the large scale galaxy distribution and the luminosity function.

1. INTRODUCTION

In 1991 we started a galaxy redshift survey over a strip of $22° \times 1°$ (plus a nearby area of $5° \times 1°$, five degrees west of the strip) in the South Galactic Pole region. The right ascension limits are 22^h30^m and 01^h20^m, at a mean declination of $-40°$ (1950). We have filled this area with a regular grid of circular fields with a diameter of 32 arcmin, corresponding to the field of view of the multifiber spectrograph OPTOPUS at the 3.6m ESO telescope.

We have selected the target objects from the Edinburgh–Durham Southern Sky Galaxy Catalogue (Heydon–Dumbleton et al. 1988). The limiting magnitude of the survey is $b_J \leq 19.4$, which optimizes the number of fibers of the spectrograph and corresponds to an effective depth of $\sim 600~h^{-1}~Mpc$.

At $z \simeq 0.1$, which corresponds to the peak of the selection function of the survey, the linear dimensions of the main strip are of the order of $110 \times 5~h^{-1}~Mpc$,
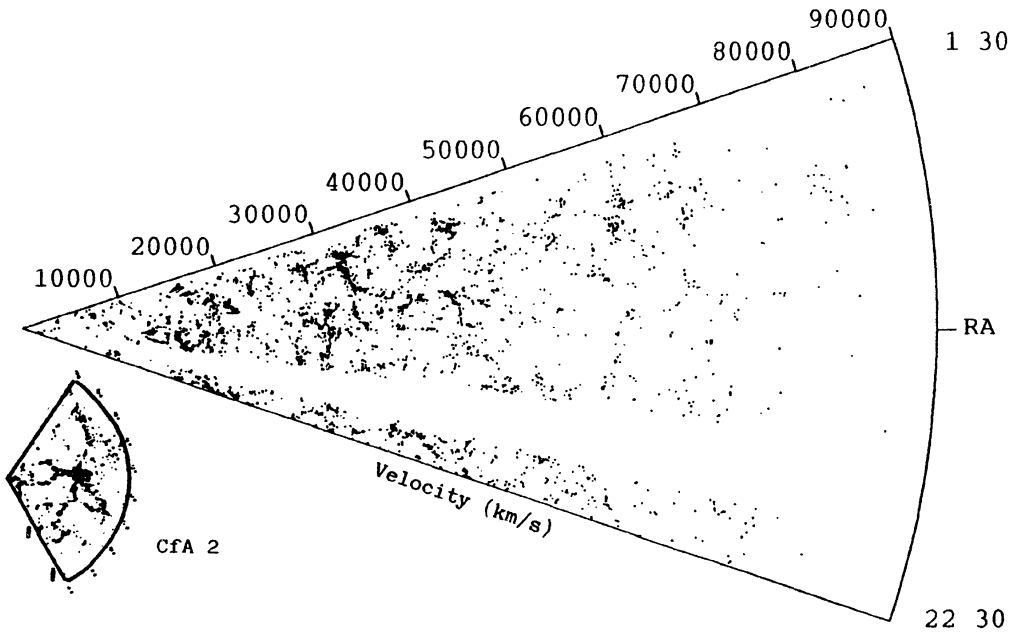
Fig.1: Wedge diagram in the region $22^h 30^m < \alpha < 1^h 30^m$ and $-40°45' < \delta < -39°45'$ of the ESP survey.

and therefore we sample a volume of $\sim 1.5 \times 10^5 \ h^{-3} \ Mpc^3$.

2. OBSERVATIONS and DATA REDUCTION

The observations have been obtained with the multifiber spectrograph OPTO-PUS at the Cassegrain focus of the ESO 3.6m telescope at La Silla. OPTOPUS has 50 fibers (2.4 arcsec diameter) which are manually plugged into holes drilled in aluminum plates. During the last observing run, in order to recover the spectra of missed, sparse objects, we also used MEFOS (at the same telescope), which has 29 fibers moved by mechanical arms over a 1 degree diameter field.

The spectra cover the wavelength range from 3730 Å to 6050 Å, with an effective resolution of about 10 Å. Spectra are flat–fielded, extracted and wavelength calibrated. Then the relative transmission of each fiber is computed by normalizing each spectrum through the flux of the OI $\lambda5577$ and Na $\lambda5891$ sky lines.

After subtraction of the average sky from the galaxy plus sky spectra (the accuracy of the sky subtraction is in the range 2–5%), the redshifts are measured by cross–correlating the spectra with a set of template stars observed by us with the same instrument. The redshifts from emission lines (when present) are also measured, as well as the equivalent width of the most common emission lines.

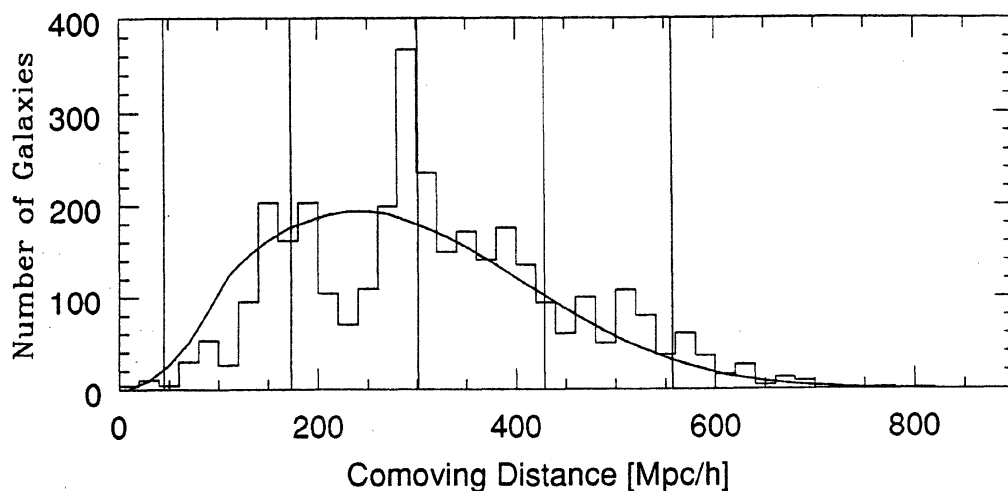The median error in velocity for the total sample is $\sim 50 \ km/s$, with a zero

Fig.2: Galaxy distribution in comoving distance ($q_0 = 0.5$). The solid line shows the expectation resulting from a uniform distribution of the galaxies in the sample. Vertical lines correspond to the position of the BEKS peaks (see text).

point accuracy of $\sim 15\ km/s$, and more than 80% of the observed fields have a redshift completeness greater than 80%.

3. LARGE–SCALE PROPERTIES

In Figure 1 it is shown the wedge diagram of the 3348 measured galaxies and on the same scale it is reported, for comparison, the wedge diagram of the CfA2 survey ($m_{lim} = 15.5$, in the northern hemisphere). From this figure it is clear that the ESP sample is not contaminated anymore by the local structures, as it happened in almost all previous surveys, and so it will be possible to use these data to obtain information on the large–scale structure unbiased by nearby inhomogeneities.

The histogram in Figure 2 shows the distribution in comoving distance ($q_o = 0.5$) of these galaxies. Note that the outstanding peak at $D \simeq 300\ h^{-1}\ Mpc$ is not due to a single galaxy cluster, but to a structure which extends over almost all the fields. The distance of this peak is almost coincident with the maximum of our selection function. Other peaks seen in Figure 2 at smaller and larger distance are due to less prominent structures, but with a similar contrast with respect to a uniform distribution.

A large fraction of galaxies ($\sim 50\%$) shows the presence of one or more emission lines (OII $\lambda 3727$, $H\beta$, OIII $\lambda 4959$ and $\lambda 5007$). These objects can be either spiral galaxies, where lines originate mostly from HII regions in the disks, or early–type galaxies undergoing a significant burst of star formation.

The large scale distribution of galaxies with emission lines is different from that of galaxies without emission lines: the observed peaks in the galaxy distribution are much less apparent in galaxies with emission lines. This suggests that either spiral galaxies are less frequent in the densest regions, thus confirming a large scale validity of the well known morphology–density relation, or starburst phenomena occur preferentially in low density environments or both. We are going to explore further this point, on the basis of quantitative estimates of densities and of a clearer definition of the structures beyond pure visual impression.

The vertical lines in Figure 2 show the location of the regularly spaced density enhancements found in a deep pencil beam survey (BEKS) in the South Galactic Pole region (Broadhurst et al. 1988, 1990). The two main peaks in our redshift distribution (at comoving distances of ~ 170 and $\sim 300 \; h^{-1} \; Mpc$) are in reasonably good agreement with the BEKS peaks and may well be part of the same structures (walls) orthogonal to the line of sight. Under this hypothesis, since the BEKS survey region is located $\sim 10°$ north of the eastern corner of the present survey, the structure at $z \simeq 0.1$ would have minimum linear dimensions of the order of $110 \times 50 \; h^{-1} \; Mpc$, comparable with the Great Wall (Geller & Huchra 1989).

Although really apparent only in the North Galactic Pole – South Galactic Pole direction, the striking "periodicity" seen in the BEKS deep survey has prompted several speculations and some controversy as well. The latter is mainly based on the criticism on the estimates of levels of statistical significance of the signal found by BEKS to be at $\lambda = 128 \; h^{-1} \; Mpc$, due to correlated structures and on the presence of aliasing of power because of the lower dimensionality of the BEKS survey (Kaiser & Peacock 1991). Even though we cover much less depth than the BEKS survey, it is worthwhile to use the present data to assess the possible presence of peaks in the power spectrum, since in our survey we gain one dimension and this is likely to affect the level of power aliasing. A careful analysis of this point is in progress.

4. THE LUMINOSITY FUNCTION

The well controlled selection of our sample and the large number of redshifts already obtained allow us to estimate for the first time the parameters of the galaxy luminosity function at magnitudes as faint as $b_J = 19.4$.

Since our database was selected in the blue–green, K–corrections are needed to compute the luminosity function even for the moderate redshifts sampled by our galaxies ($z \leq 0.2$). The functional forms of the K–correction as a function of redshift (Shanks et al. 1984) obviously requires the knowledge of the morphological type of each galaxy, which is not available for our fainter galaxies. To overcome this problem, we have adopted the following statistical approach. First, we have assumed that the percentages of late– and early–type galaxies in our sample are approximately the same as those observed in brighter and nearer samples (Shanks et al. 1984) then we have applied the K–correction appropriate for a late–type galaxy to all galaxies showing emission lines. Finally, we have randomly assigned a morphological type to the remaining galaxies in such a way as to obtain the assumed ratio of late and early types in the total sample.

Following the STY method (Sandage et al. 1979) we have then derived the parameters of the Schechter functional form of the luminosity function, through a maximum likelihood technique. The best fit parameters are $\alpha = -1.16$ and $M_{b_J}^* = -19.56$. In order to estimate the maximum amount of uncertainty induced
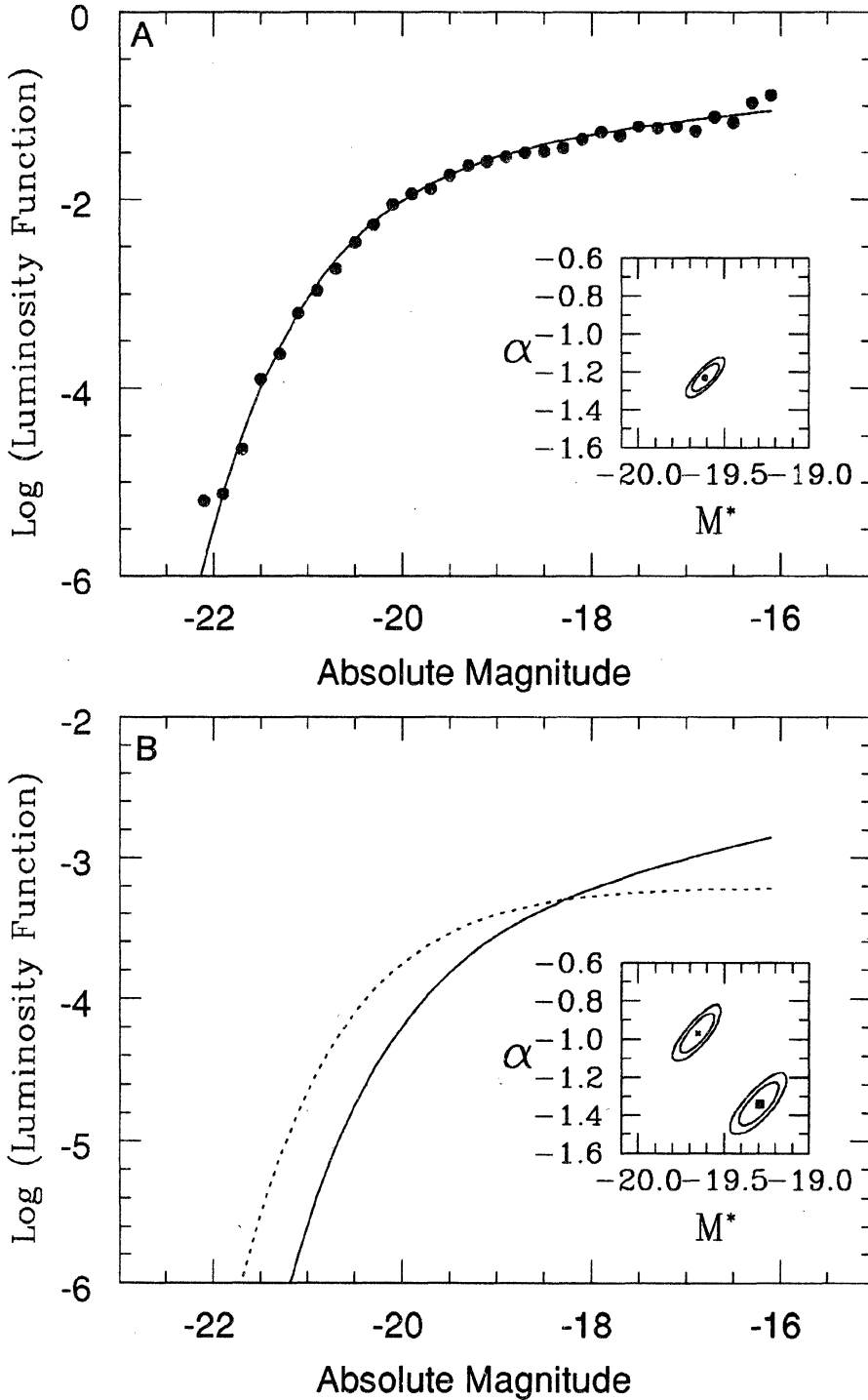
Fig.3: a) Galaxy luminosity function for the total sample: solid circles have been computed using a modified version of the C–method and the normalization is arbitrary. b) Normalized luminosity functions for galaxies with emission lines (squares and solid line) and without emission lines (triangles and dotted line).

by our "statistical" K–correction scheme, we have also computed the two parameters of the luminosity function with the extreme assumptions that all galaxies are either ellipticals or spirals. The best fit parameters obtained in these way are $\alpha = -1.23$, $M_{b_J}^* = -19.78$ and $\alpha = -1.14$, $M_{b_J}^* = -19.48$, respectively.

Figure 3a shows the luminosity function (with arbitrary normalization) obtained for our sample: the solid line corresponds to the Schechter functional form obtained through the STY method, while the solid circles have been determined through a modified version of the non–parametric C–Method (Lynden–Bell 1971). The fit is based on 3311 galaxies brighter than $M_{b_J} = -16$ and the 68% and 95% confidence ellipses for α and $M_{b_J}^*$ are shown in the inset.

Finally in Figure 3b we show the normalized luminosity functions computed for galaxies with and without emission lines: it is clear that the two functions differ at a very high confidence level, thus suggesting that these two classes of galaxies really represent two different "populations".

The next steps are the refinement of the K–correction procedure, varying the morphological mix as a function of redshift, and the estimate of the luminosity function normalization.

Acknowledgements

REFERENCES

Broadhurst, T.J., Ellis, R.S., Shanks, T., 1988, *MNRAS* 235, 827

Broadhurst, T.J., Ellis, R.S., Koo, D.C., Szalay, A.S., 1990, *Nature* 343, 726

Geller, M.J., Huchra, J.P., 1989, *Science* 246, 897

Heydon–Dumbleton, N.H., Collins, C.A., MacGillivray, H.T., 1988, in *Large–Scale Structures in the Universe*, ed. W. Seitter, H.W. Duerbeck and M. Tacke (Springer–Verlag), p. 71.

Kaiser, N, Peacock, J.A., 1991, *ApJ* 379, 482

Lynden–Bell, D., 1971, *MNRAS* 155, 95

Sandage, A., Tamman, G., Yahil, A., 1979, *ApJ* 232, 252

Shanks, T., Stevenson, P.R.F., Fong, R., MacGillivray, H.T., 1984, *MNRAS* 206, 767